Bioconjugate Chemistry

pubs.acs.org/bc Article

Combinatorial Library of Cyclic Benzylidene Acetal-Containing pH-Responsive Lipidoid Nanoparticles for Intracellular mRNA Delivery

Yamin Li, Raissa Li,[#] Anirban Chakraborty,[#] Roza Ogurlu, Xuewei Zhao, Jinjin Chen, and Qiaobing Xu*

Cite This: *Bioconjugate Chem.* 2020, 31, 1835−1843 Read Online

ACCESS | Metrics & More | Article Recommendations | Supporting Information

ABSTRACT: Lipidoid nanoparticles have been demonstrated to be effective for intracellular delivery of small molecule drugs, proteins, and nucleic acids. Stimuli-responsive lipidoid nanoparticles are able to further improve delivery efficacy and reduce carrier-induced toxicity. Our group previously developed reduction and photoresponsive combinatorial libraries of lipidoid nanoparticles for small molecule and biologics delivery. Herein, we describe the synthesis, characterization, and intracellular mRNA delivery application of a new library of pH-responsive lipidoid nanoparticles. The acid-degradable cyclic benzylidene acetal-containing cationic lipidoids (R-O16CBA) were synthesized through a multistep reaction and characterized by NMR and MS. The acid-triggered degradation of lipidoids was studied using NMR, MS, DLS, and TEM. The results revealed that the R-O16CBA lipidoid can be completely degraded at pH 5. The R-O16CBA lipidoid nanoparticles were then fabricated with different formulations of DOPE and cholesterol and tested *in vitro* for intracellular mRNA delivery.

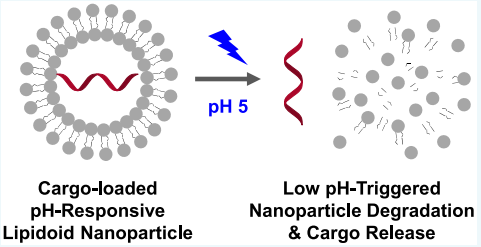

INTRODUCTION

The combinatorial library strategy has been shown to be effective for the development of cationic lipid-like (lipidoid) nanoparticles (LNPs) for drug delivery.[1−3] Lipidoid molecules with various hydrophilic amine heads and hydrophobic tails have been synthesized and used to deliver small molecules,[4−6] proteins and peptides,[7−10] ribonucleoproteins (RNP),[11−13] and nucleic acids (mRNA, siRNA, ASO, pDNA, etc.),[14−17] both *in vitro* and *in vivo*. Lipidoid molecular design and nanoparticle supramolecular structure optimization strategies have achieved better delivery performances by improving delivery specificity, enhancing efficacy, and reducing side effects.[18−20] In order to further refine molecular structure design, we have incorporated functional groups with stimuli-responsive degradable features into combinatorial lipidoid molecules.

Our group first reported a library of reduction-responsive disulfide bond-containing lipidoid nanoparticles that can be degraded in the presence of glutathione (GSH) and other intracellular reducing agents.[21,22] These lipidoids were used for siRNA and protein delivery. The concept of a stimuli-responsive combinatorial lipidoid library was further expanded from a biochemical trigger to a physical/external trigger. This was achieved through the integration of the *o*-nitrobenzyl ester group into our lipidoid tail structures.[4] Photodegradable lipidoid nanoparticles were then fabricated and used for small molecule drug delivery.

Each library of stimuli-responsive lipidoids has its own unique physicochemical properties. Creating and expanding these libraries helps to enrich our molecular toolbox for nanodrug delivery applications. In this article, we report a new combinatorial library of biochemical signal-responsive lipidoid nanoparticles. Acid-cleavable acetal, hydrazone, and ester groups have been used to induce pH sensitivity for various materials, such as polymers,[23−26] lipids,[27,28] and organic−inorganic hybrid nanoparticles.[29,30] Each linkage system has its own advantages and disadvantages. Additionally, their hydrolytic stabilities at physiological pH and acid labilities/sensitivities can be finely tuned by structural modifications. The molecular features and applications of these acid-labile conjugate chemistries have been summarized in recent reports.[31−34] In this study, we incorporated a pH-sensitive cyclic benzylidene acetal (CBA) group, which has shown extraordinary stability at physicological pH and mild acid-triggered degradation feature, into the tail structures of a combinatorial library of lipidoids.[23,35,36] The acid-degradable tail, O16CBA, was first synthesized through a multistep reaction. The cationic lipidoids, R-O16CBA, were then synthesized through the Michael addition reaction using commercially available amine head groups and the acrylate-containing O16CBA tails. After fabrication of the lipidoid nanoparticles through self-assembly procedures, the degradation of lipidoid molecules and subsequent dissociation of nanoparticles triggered by low pH were examined. Finally, different nano-

Received: May 12, 2020
Revised: June 7, 2020
Published: June 10, 2020

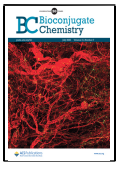

https://dx.doi.org/10.1021/acs.bioconjchem.0c00295
Bioconjugate Chem. 2020, 31, 1835−1843

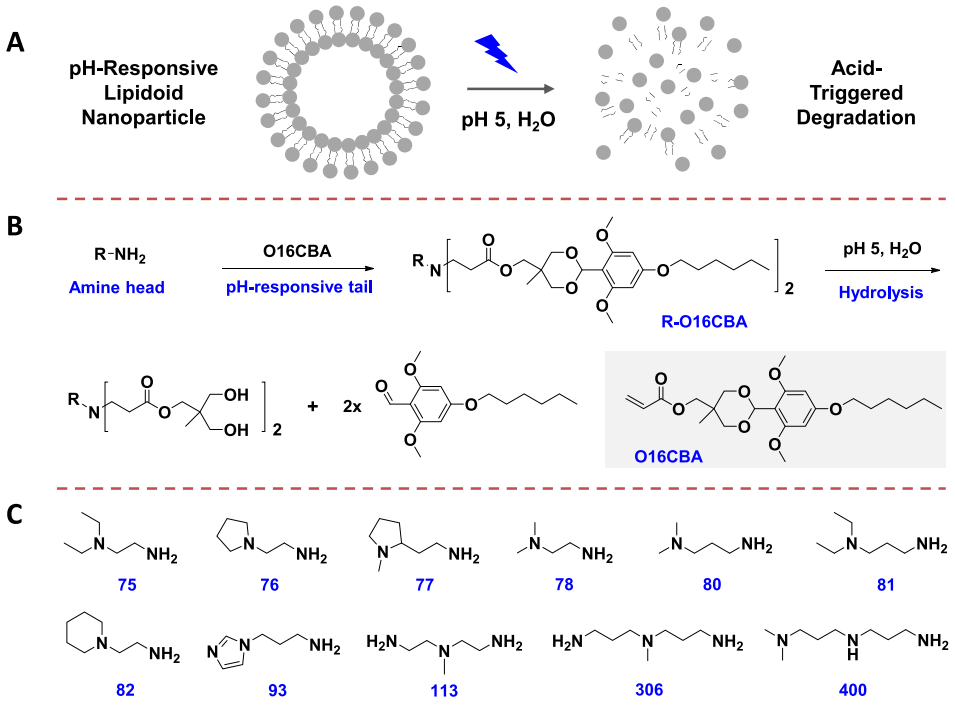

Figure 1. Combinatorial library of pH-responsive lipidoid nanoparticles. (A) Schematic illustration of the acid-triggered degradation of lipidoid nanoparticles. (B) Synthetic route and acidic pH-triggered hydrolysis reaction of R-O16CBA lipidoids. (C) Chemical structures of amine head groups.

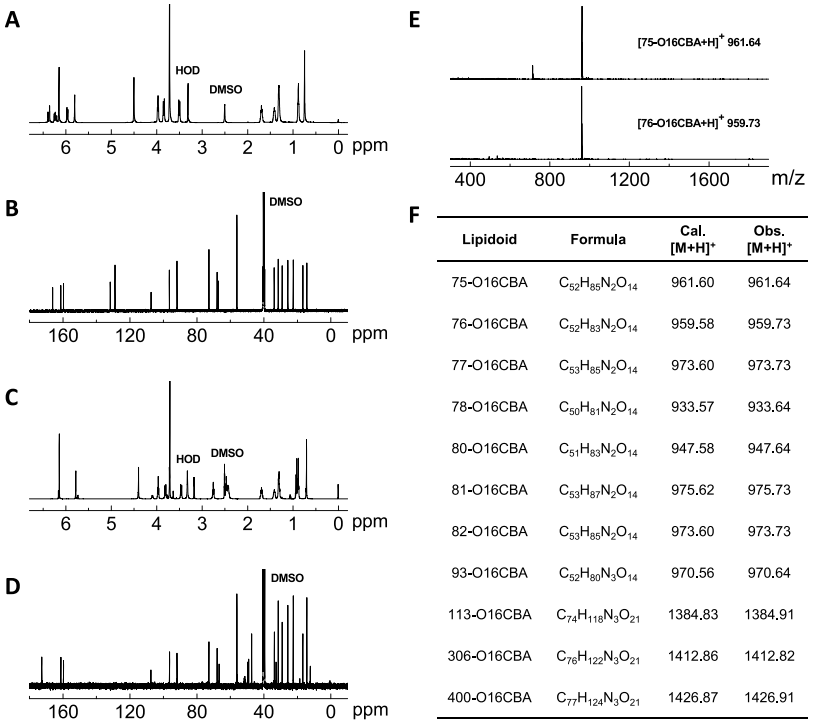

F

Lipidoid	Formula	Cal. $[M+H]^+$	Obs. $[M+H]^+$
75-O16CBA	$C_{52}H_{85}N_2O_{14}$	961.60	961.64
76-O16CBA	$C_{52}H_{83}N_2O_{14}$	959.58	959.73
77-O16CBA	$C_{53}H_{85}N_2O_{14}$	973.60	973.73
78-O16CBA	$C_{50}H_{81}N_2O_{14}$	933.57	933.64
80-O16CBA	$C_{51}H_{83}N_2O_{14}$	947.58	947.64
81-O16CBA	$C_{53}H_{87}N_2O_{14}$	975.62	975.73
82-O16CBA	$C_{53}H_{85}N_2O_{14}$	973.60	973.73
93-O16CBA	$C_{52}H_{80}N_3O_{14}$	970.56	970.64
113-O16CBA	$C_{74}H_{118}N_3O_{21}$	1384.83	1384.91
306-O16CBA	$C_{76}H_{122}N_3O_{21}$	1412.86	1412.82
400-O16CBA	$C_{77}H_{124}N_3O_{21}$	1426.87	1426.91

Figure 2. Characterization of O16CBA tail and R-O16CBA lipidoids. (A) ^{1}H and (B) ^{13}C NMR spectra of O16CBA tail. (C) ^{1}H and (D) ^{13}C NMR spectra of 75-O16CBA lipidoid. (E) ESI-MS spectra of 75-O16CBA and 76-O16CBA. (F) Summary of chemical formulas and calculated and observed molecular weights of R-O16CBA lipidoids.

formulations with acid-degradable R-O16CBA, DOPE, and cholesterol were tested for *in vitro* mRNA delivery (Figure 1).

RESULTS AND DISCUSSION

Lipidoid Synthesis. The pH-responsive cyclic benzylidene acetal-containing hydrophobic tail, O16CBA, was first synthesized through a multistep reaction (Figure S1). Chemical structures of O16CBA (Figure 2A and B) and its precursors (Figures S2 and S3) were confirmed by NMR analysis.[35] A combinatorial library of cationic lipidoids was then synthesized through the Michael addition reaction by reacting acrylate-containing O16CBA tails with commercially available amine-containing head groups (75, 76, 77 etc.; Figure 1B and C).[21]

https://dx.doi.org/10.1021/acs.bioconjchem.0c00295
Bioconjugate Chem. 2020, 31, 1835−1843

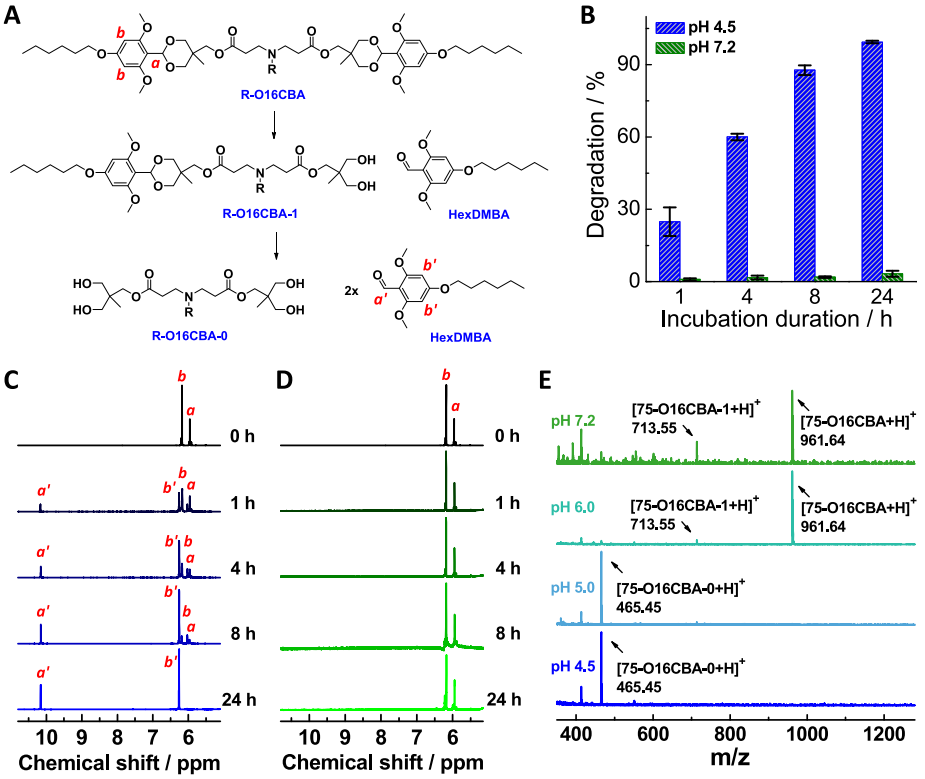

Figure 3. Acid-triggered lipidoid degradation. (A) Schematic illustration of the acid-induced hydrolysis reaction and tail cleavage of O16CBA lipidoids. (B) Degradation efficacy of the cyclic benzylidene acetal group in 75-O16CBA lipidoids at pH 4.5 and 7.0 for different incubation durations. ^{1}H NMR spectra of 75-O16CBA lipidoids under (C) pH 4.5 and (D) pH 7.2. (E) ESI-MS spectra of 75-O16CBA LNPs 24 h after incubation at pH 7.2, 6.0, 5.0, and 4.5.

Lipidoids were named R-O16CBA (where R represents the amine number) and chemical structures were confirmed by NMR (Figure 2C and D) and ESI-MS spectra (Figures 2E and 4S). The summarized MS data (Figure 2F) showed that the calculated and observed molecular weights of the O16CBA lipidoid library were consistent, indicating that the O16CBA-based lipidoids were successfully synthesized. It should be noted that analogs of O16CBA can be synthesized through the same method by using different benzaldehyde derivatives and haloalkanes as reactants (Figure S1).[32] This can be useful for introducing new functional groups or further optimizing the delivery performances of lipidoid nanoparticles as nanocarriers.

The cyclic benzylidene acetal moiety in the lipidoid tail can be cleaved through a hydrolysis reaction facilitated by acid.[27,32,35] It has been previously reported that 2,4,6-trimethoxyphenyl group-containing cyclic acetal groups can be readily degraded at pH 5.[23,35] The R-O16CBA lipidoids synthesized in this study were thus expected to degrade in mild acidic conditions, dissociating the self-assembled nanoparticles (Figure 1A and B).

pH-Responsiveness of R-O16CBA Lipidoids. In this library, lipidoids containing two tails, such as 75-O16CBA and 76-O16CBA, have both their tails cleaved through acid degradation. During this process, the products R-O16CBA-1, R-O16CBA-0, and HexDMBA can form (Figure 3A). Lipidoids containing more than two tails (113-, 306-, and 400-O16CBA) can form more products after degradation. Using characteristic peaks shown in the ^{1}H NMR spectrum of the cyclic benzylidene acetal/aldehyde moiety on intact lipidoids and degradation products, the acid-triggered lipidoid degradation process could be studied in real time. Following a previously established procedure,[27] the hydrolysis reactions of 75-O16CBA lipidoids were examined at 37 °C and pH 7.2 or 4.5. As shown in Figure 3B, the degradation of cyclic benzylidene acetal groups was determined to be 25%, 60%, 88%, and 99% after 1, 4, 8, and 24 h of incubation at a pH of 4.5. The result indicates that most of the tail groups in 75-O16CBA lipidoids were cleaved after 8 h of treatment, and almost all were degraded after 24 h. This is consistent with previous reports outlining how 2,4,6-trimethoxyphenyl-containing cyclic acetal groups are highly degradable under acidic conditions.[35] In comparison, only 1.9% and 3.3% acetal bond degradation occurred for 75-O16CBA lipidoids after 8 and 24 h incubated at pH 7.2. The characteristic proton signals indicated in Figure 3A can be observed in the ^{1}H NMR spectra of 75-O16CBA at pH 4.5 (Figure 3C). No peak shift (protons on substituted phenyl group) or new peak generation (proton on aldehyde group) was observed in the spectra of lipidoids in pH 7.2 solution (Figure 3D) at various incubation time intervals (0, 1, 4, 8, and 24 h). Using the ^{1}H NMR measurements, it can be concluded that the O16CBA tail is stable under pH 7.2 and can be degraded under pH 4.5 after 24 h of incubation at 37 °C.

The acid-triggered lipidoid degradation was further confirmed by ESI-MS. 75-O16CBA, 76-O16CBA, and 77-O16CBA lipidoid nanoparticles were prepared and incubated at 37 °C in aqueous solutions with pH values of 7.2, 6.0, 5.0, and 4.5, respectively. After 24 h, the LNP aqueous solutions were diluted with methanol containing 0.5% acetic acid and examined by ESI-MS. As shown in Figure 3E, a peak representing intact 75-O16CBA ($[M + H]^+$; m/z 961.64) and a small peak representing 75-O16CBA-1 (m/z 713.55) were observed in the solutions of pH 7.2. It should be noted that the presence of 75-O16CBA-1 in the pH 7.2 solution was most likely due to the degradation

https://dx.doi.org/10.1021/acs.bioconjchem.0c00295
Bioconjugate Chem. 2020, 31, 1835−1843

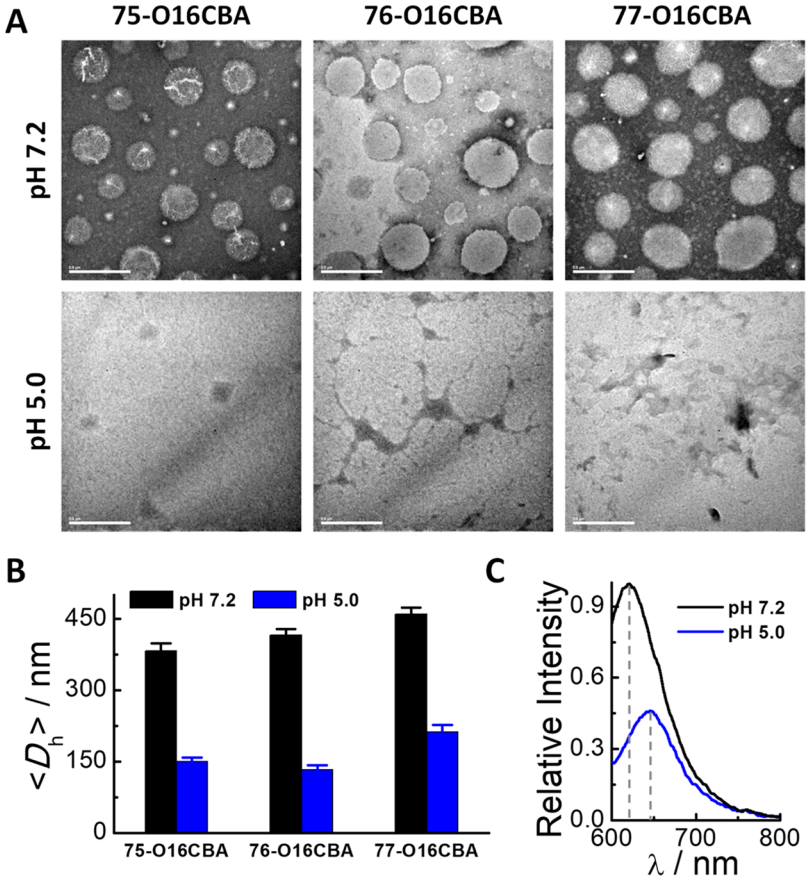

Figure 4. Acid-triggered nanoparticles degradation. (A) TEM images (scale bar = 500 nm) and (B) average hydrodynamic diameters of R-O16CBA LNPs in neutral (pH 7.2) and acidic (pH 5.0) solutions. (C) Fluorescence emission spectra of NR/75-O16CBA LNPs in pH 7.2 and 5.0 solutions.

induced by acid from the MS test, as the ^{1}H NMR did not show the generation of 75-O16CBA-1 or aldehyde byproducts after 24 h of incubation at pH 7.2 (Figure 3D). The ESI-MS of 75-O16CBA incubated at pH 6.0 showed similar results to those at pH 7.2, since both the intact 75-O16CBA and a small peak of 75-O16CBA-1 were observed. Under pH 4.5, the product 75-O16CBA-0 was detected, and no 75-O16CBA-1 or intact 75-O16CBA was observed. This indicates that the degradation of 75-O16CBA was nearly complete after 24 h at pH 4.5, which is consistent with the ^{1}H NMR measurement (Figure 3B). Samples treated with pH 5.0 conditions revealed very similar results as those at pH 4.5. Furthermore, as shown in Figures S5 and S6, the same patterns were observed for two other lipidoids (76-O16CBA and 77-O16CBA). Our observation is consistent with previously reported results regarding cyclic benzylidene acetal-containing systems.[23,35] Overall, it was concluded that the O16CBA lipidoids can be readily degraded in acidic conditions at or below pH 5.0, but remain stable at neutral pH around 7.2.

Acid-Induced Degradation of O16CBA Lipidoid Nanoparticles. The morphological change of O16CBA LNPs under acid-induced degradation was studied using TEM and DLS. In this study, 75-O16CBA LNPs were fabricated using a self-assembly procedure. Through TEM examination, it was confirmed that spherical nanoparticles with average sizes of 315 nm formed in the pH 7.2 solution (Figure 4A). These nanoparticles seem to be vesicular structures/liposomes and similar morphologies have also been observed previously in our and others' studies.[8,37−39] Due to the packing parameters of the lipidoid molecules and the self-assembly procedures that were employed, almost all of our previously studied combinatorial lipidoid nanoparticles have the liposomal structures.[4,8,21] The supramolecular characteristics of lipidoid nanoparticles (e.g., morphology, size, etc.) are supposed to be reliant on both the chemical structures of lipidoid mlecules and assembly conditions.[40,41] The size and distribution of lipidoid nanoparticles can also be further optimized using microfluidics, mechanical extrusion, and other techniques.[42,43]

After 24 h incubation at pH 5.0, the lipidoid nanoparticles were disrupted and amorphous aggregates around 130 nm resulted (Figure 4A). The same acid-triggered morphological transformations were also observed in 76-O16CBA and 77-O16CBA LNPs with TEM images (Figure S7). DLS measurements further indicated size variations after acid treatment. The hydrodynamic diameter of 75-O16CBA decreased from 382 to 150 nm after 24 h of incubation in pH 5.0 solution (Figure 4B). Decrease in average hydrodynamic size was also observed for 76- and 77-O16CBA, which was consistent with the TEM observation results. The hydrodynamic size of R-O16CBA measured by DLS was larger than the average size calculated from TEM images. This could be due to the fact that the TEM images were taken under dry status.[8,44] Following previously reported procedures,[4,45] a microenvironment polarity-sensitive fluorescent dye (Nile red) was incorporated into the hydrophobic lipidoid bilayer membrane of 75-O16CBA LNPs. Nile red has bright fluorescence emission in the nonpolar environment such as lipidoid bilayer, and reduced fluorescence in polar or aqueous solution. A decrease in fluorescence emission intensity (ca. 54%) and a red-shift in maximum emission peaks

https://dx.doi.org/10.1021/acs.bioconjchem.0c00295
Bioconjugate Chem. 2020, 31, 1835−1843

(from 619 to 646 nm) of NR/75-O16CBA was observed after 24 h of incubation at pH 5.0 (Figure 4C). This indicated that the microenvironment variation and nanoparticle dissociation occurred after the acid treatment. Overall, the ^{1}H NMR, MS, TEM, DLS, and fluorescence measurements demonstrated the acid-triggered degradation of R-O16CBA lipidoid molecules as well as the resulting disruption of nanoparticle structures.

R-O16CBA LNPs for mRNA Delivery. We explored the possibility of using R-O16CBA molecules as the active lipidoids for intracellular mRNA delivery.[46,47] In this study, different formulations were prepared. As shown in Table 1, R-O16CBA LNPs contain R-O16CBA only; R-O16CBA-F1 LNPs contain R-O16CBA, cholesterol, and DOPE at a weight ratio of 4/1/1; R-O16CBA-F2 LNPs contain R-O16CBA, cholesterol, and DOPE at a weight ratio of 4/1/4. Cholesterol and DOPE were added because previous studies have shown that these helper lipids can increase the stabilization of nanoparticles, membrane infusion, and cellular internalization.[18,48,49] The nanoparticle formulations with R-O16CBA/cholesterol/DOPE = 4/4/1 (weight ratios) were also prepared, but all formulations immediately precipitated after dialysis procedures regardless of the amine headgroup. This is most likely due to the hydrophobicity of cholesterol. As a result of this stability issue, the O16CBA/cholesterol/DOPE = 4/4/1 (weight ratios) formulation was not further tested.

Table 1. Codes and Parameters of Lipidoid Nanoparticle Formulations Used in This Study

	weight ratio		
code	lipidoid	cholesterol	DOPE
R-O16CBA	4	0	0
R-O16CBA-F1	4	1	1
R-O16CBA-F2	4	1	4

GFP mRNA was loaded into different nanoparticle formulations by mixing mRNA and LNPs in PBS buffer (R-O16CBA/mRNA = 10/1; weight ratio). Our previous studies have shown that an increase in LNPs hydrodynamic sizes is usually observed after cargo molecules are loaded. Most of our combinatorial LNPs have shown great stability during storage.[8,50] Furthermore, the stability of LNPs can be further improved by adding small and macromolecular excipients (cholesterol, DOPE, PEG-DSPE etc.) into the formulations.[8] It should be noted that in all of the following studies, freshly prepared LNPs were used unless otherwise noted. The mRNA and LNPs were added to HeLa cells, and the delivery efficiencies were determined using flow cytometry after 24 h of incubation ([R-O16CBA] = 7.4 μg/mL; [GFP mRNA] = 0.74 μg/mL; exposure duration = 24 h). Intracellular mRNA delivery efficiency was represented by the percentage of GFP$^+$ cells. Commercially available cationic transfection reagent, Lpf2k, was used as a positive control. Untreated HeLa cells and HeLa cells treated with naked GFP mRNA were used as negative controls. As shown in Figure 5, both untreated cells and naked mRNA-treated cells induced a negligible percentage of GFP$^+$ HeLa cells (<1%). On the other hand, Lpf2k was highly efficient in mRNA delivery as ~91% GFP$^+$ cells were recorded.

It was discovered that the neutral helper lipids (cholesterol and DOPE) in R-O16CBA formulations played an essential role in mRNA delivery. Without helper lipids, the delivery efficiencies were rather low, as eight of the LNP formulations (75-O16CBA and 76-O16CBA etc.) had efficiencies below 15%. Two lipidoid nanoparticles, 113-O16CBA and 306-O16CBA, induced 29% and 44% GFP$^+$ cells, respectively, while the most active 400-O16CBA induced 68% GFP$^+$ cells. The outperformance of lipidoids with more than two tails (113-, 306-, and 400-O16CBA) compared to lipidoids with two tails (75-O16CBA etc.) for nucleic acid delivery is consistent with previous reports and merits further study.[20]

The addition of helper lipids greatly improved LNP delivery efficacy, with multiple LNPs achieving GFP expression comparable to that of Lpf2k. In the library of R-O16CBA-F1 formulations, all LNPs, except for 93-O16CBA-F1 (~2% GFP$^+$ cells), showed higher efficacies than their corresponding R-O16CBA formulations. Nine of the R-O16CBA-F1 formulations had >50% delivery efficiency, with 81-O16CBA-F1 being the highest in producing ~93% GFP$^+$ cells. Other top formulations such as 76-, 77-, 113-, 306-, and 400-O16CBA-F1 induced delivery efficacies of 78−83%.

We then investigated the effects of increasing the amount of helper lipids on mRNA delivery. As we have mentioned, the formulations with R-O16CBA/cholesterol/DOPE at 4/4/1 weight ratio were not stable. Therefore, formulations with R-O16CBA/cholesterol/DOPE at a weight ratio of 4/1/4 were fabricated and tested (R-O16CBA-F2). As shown in Figure 5, except for the 93-O16CBA-F2 and 400-O16CBA-F2, all other LNPs had higher efficacies than R-O16CBA. Compared to the R-O16CBA-F1 LNPs, the delivery efficacies of R-O16CBA-F2 were slightly lower (except for 75- and 78-O16CBA-F2). 81-

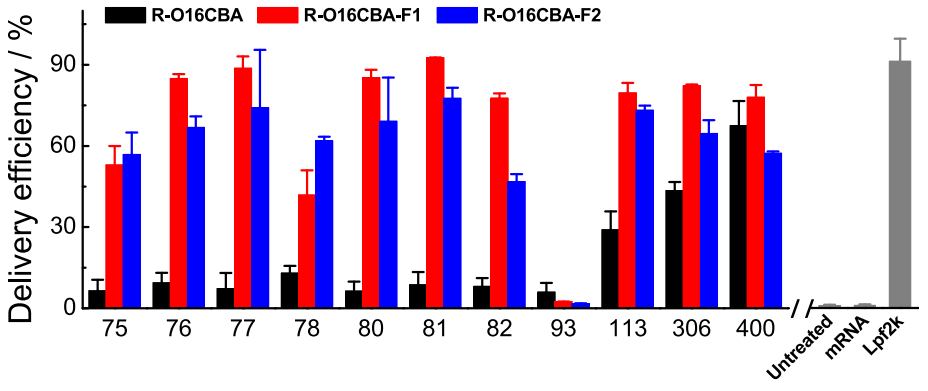

Figure 5. Intracellular GFP mRNA delivery efficacies of R-O16CBA LNP formulations (R-O16CBA, R-O16CBA-F1, and R-O16CBA-F2) to HeLa cells. Lpf2k and naked mRNA were used as positive and negative controls, respectively. [R-O16CBA] = 7.4 μg/mL; [GFP mRNA] = 0.74 μg/mL; exposure duration = 24 h.

https://dx.doi.org/10.1021/acs.bioconjchem.0c00295
Bioconjugate Chem. 2020, 31, 1835−1843

O16CBA-F2 was determined to be the most efficient in this formulated library as ~78% GFP$^+$ cells were recorded. Once again, 113-, 306-, and 400-O16CBA-F2 were still among the top LNPs, as their delivery efficacies were determined to be 57−73%.

Overall, the addition of helper lipids can improve most LNP delivery efficacies, corroborating previous studies.[11,18,51] R-O16CBA-F2 LNPs, which had higher DOPE content, had comparable or slightly lower efficacies than R-O16CBA-F1 LNPs. Further studies will focus on the R-16CBA-F1 LNPs, taking delivery efficacy and fabrication costs into consideration. In addition, 81-O16CBA-F1 and -F2 were determined to be the most efficient in the two formulation libraries, and three-tailed LNPs performed well both with and without helper lipids. We have recently shown that factors like the chemical structure of lipdoids, formulation components, supramolecular structure of lipidoid nanoparticles, and cargo species play important roles in determing cell-type specificity and overall delivery efficacy.[8,11,50] Future studies will also examine in depth the selectivity and efficiency of the R-O16CBA-based nanoparticle formulations for mRNA delivery to various cell types both *in vitro* and *in vivo*.

Cytotoxicity Test. As discussed above, some of the R-O16CBA formulations achieved comparable mRNA delivery efficacies to that of the commercial reagent Lpf2k. Besides efficacy, the biocompatibility of carriers should also be examined. Although Lpf2k is highly efficient, previous research indicated it is also toxic.[8,21] In this context, the cytotoxicities of four successful R-O16CBA LNPs, namely, one two-tailed lipidoid (81-O16CBA) and three multiple-tailed lipidoids (113-, 306-, and 400-O16CBA) were tested using the MTT assay ([lipidoid] = 7.4 μg/mL; exposure duration = 24 h). It should be noted that our previous studies have shown that the cytotoxicity of combinatorial lipidoid nanoparticle formulations generally depend primarily on the synthetic active lipidoids.[11] The addition of helper lipids like cholesterol and DOPE would result in very similar or slightly lower cytotoxicity of the formulations, which is reasonable considering the excellent cell compatibility of cholesterol and DOPE, etc.[11] As shown in Figure 6, although Lpf2k is highly efficient for mRNA delivery, it is also rather toxic, as only ~53% of cells were viable after delivery. On the other hand, the newly developed R-O16CBA LNPs were less toxic under the same conditions. 306- and 400-O16CBA had ~70% cell viabilities, and 81- and 113-O16CBA had >90% cell viabilities. The very low toxicities of 81- and 113-O16CBA, coupled with their high delivery efficiencies, make them especially promising candidates for further study.

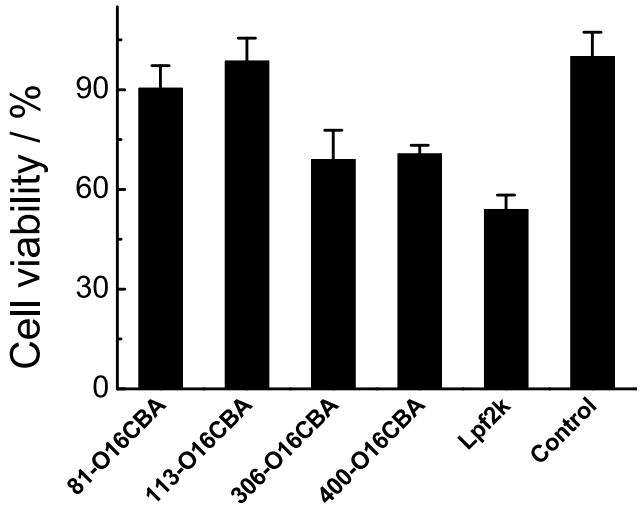

Figure 6. Cytotoxicity test of R-O16CBA LNPs and Lpf2k ([lipidoid] = 7.4 μg/mL; exposure duration = 24 h). Untreated HeLa cells were used as negative controls.

CONCLUSION

In summary, a new combinatorial library of acid-degradable lipidoids, R-O16CBA, was synthesized. The acid-triggered degradation of lipidoid molecules and nanoparticles were studied, and the possibility of using R-O16CBA LNPs for intracellular mRNA delivery was demonstrated. Some of the newly developed formulations achieved delivery efficiencies comparable to that of Lpf2k. Further studies revealed that the top acid-degradable lipidoids were more biocompatible than Lpf2k. Future experiments will incorporate new head and tail structures, optimize *in vitro* and *in vivo* mRNA delivery performances, and explore therapeutic applications for *ex vivo* or *in vivo* use.[52,53]

EXPERIMENTAL SECTION

Materials and Instruments. All chemicals and solvents used for lipidoid synthesis were purchased from Millipore-Sigma and used without purification unless otherwise noted. ^{1}H and ^{13}C NMR spectra were collected on a Bruker AVIII 500 MHz NMR spectrometer. ESI-MS spectra were collected on a Finnigan LTQ Mass Spectrometer using methanol as a solvent (0.5% acetic acid; v/v). Hydrodynamic sizes of nanoparticles were measured by a Brookhaven Zeta-PALS particle size analyzer. TEM images were taken on a FEI Technai Transmission Electron Microscope. GFP mRNA transfected cells were analyzed with an Invitrogen Attune NxT Flow Cytometer, and data was analyzed using FlowJo software.

Synthesis of O16CBA. The synthetic route for cyclic benzylidene acetal-containing hydrophobic tail, O16CBA, is shown in Figure S1.

4-Hydroxy-2,6-dimethoxybenzaldehyde (HDMBA; 5.1 g, 28.0 mmol) was dissolved in acetone (100 mL). Potassium carbonate (4.6 g, 33.3 mmol) was added followed by 1-bromohexane (6.8 g, 41.2 mmol) with continuous stirring. The reaction was maintained at 55 °C for 24 h. The mixture was cooled to room temperature and filtered with filter paper. The solvent was then removed through rotary evaporation, and the product was purified by silica gel column chromatography, with hexane and ethyl acetate as the mobile phase. HexDMBA was obtained as a white solid (5.2 g; yield ~70%) and the structure was confirmed by ^{1}H NMR (Figure S2).

HexDMBAH was synthesized using a similar procedure reported previously.[35] Briefly, HexDMBA (5.2 g, 19.5 mmol) and 1,1,1-tris(hydroxymethyl)ethane (6.7 g, 55.9 mmol) were dissolved in anhydrous tetrahydrofuran (200 mL). 5 Å molecular sieves (30 g) and *p*-toluenesulfonic acid (0.44 g, 2.56 mmol) were then added. The reaction mixture was stirred at room temperature for 12 h, molecular sieves were filtered out, and solvent was removed via rotary evaporation. HexDMBAH was purified by silica gel column chromatography, with hexane and ethyl acetate as the mobile phase. HexDMBAH was recovered as a white solid (5.4 g; yield ~75%), and its structure was confirmed by ^{1}H NMR (Figure S3).

HexDMBAH (5.4 g, 14.7 mmol) was dissolved in dichloromethane (~150 mL) followed by triethylamine (2.2 g, 22.1

https://dx.doi.org/10.1021/acs.bioconjchem.0c00295
Bioconjugate Chem. 2020, 31, 1835−1843

mmol). The solution was cooled in an ice bath for 15 min, and acryloyl chloride (2.00 g, 22.1 mmol) was slowly added dropwise. The reaction mixture was allowed to warm to room temperature and was stirred for 12 h. After silica gel column chromatography purification, with the same mobile phase as previously described, O16CBA was obtained as a white solid (4.5 g; yield ~73%). Its structure was confirmed using ^{1}H and ^{13}C NMR (Figure 2A and B).

Synthesis of O16CBA-Tailed Lipidoids. Lipidoids were synthesized from the O16CBA tail and amine heads via the Michael addition reaction, using our previously reported procedure.[8] To synthesize 75-O16CBA etc., amines (75, 76, 77, 78, 80, 81, 82, and 93) were mixed with O16CBA at a 1/2.2 molar ratio. To synthesize 113-O16CBA, amines (113, 306, and 400) were mixed with O16CBA at a 1/3.3 molar ratio. These mixtures were placed in Teflon-lined glass screw-top vials for 48 h at 70 °C with continuous stirring. The mixtures were cooled to room temperature and diluted with dichloromethane. The crude products were purified using a Teledyne ISCO chromatography purification system, with dichloromethane and methanol as the mobile phase. The lipidoids were characterized by ^{1}H NMR, ^{13}C NMR (Figure 2C and D), and ESI-MS (Figures 2E and S4).

Fabrication of Lipidoid Nanoparticles. The lipidoid nanoparticles without helper lipids (i.e., cholesterol and DOPE) were prepared by dissolving pure O16CBA lipidoids (75-O16CBA etc.) in ethanol. Water was added as the selective solvent to trigger the self-assembly process with 10 min of sonication in an ultrasonic water bath. This was followed by dialysis (MWCO 3.5 kDa; Slide-A-Lyzer dialysis cassette; ThermoFisher Scientific) to remove the ethanol. The lipidoid nanoparticles with cholesterol and DOPE were prepared by dissolving a precalculated amount of O16CBA lipidoids, cholesterol, and DOPE (O16CBA lipidoid/cholesterol/DOPE = 4/1/1 or 4/1/4; weight ratio) in ethanol and then water. This was again followed by sonication and dialysis.

GFP mRNA- (purchased from TriLink) loaded lipidoid nanoparticles were fabricated by mixing lipidoid nanoparticles (with or without helper lipids) and mRNA in PBS with a weight ratio of 10/1 (R-O16CBA lipidoid/mRNA). The mixture was incubated at room temperature for 15 min before use.

Intracellular Delivery of mRNA. 48-well plates were seeded with HeLa cells at an initial concentration of 20 k cells per well dispersed in 250 μL of DMEM cell culture media and incubated for 24 h. Twenty microliters of the mRNA-loaded lipidoid nanoparticles was then added into each well. The cells were incubated for another 24 h at 37 °C and 5% CO_2 prior to flow cytometry analysis.

MTT Assay. 96-well plates were seeded with HeLa cells at an initial concentration of 5000 cells per well dispersed in 100 μL of DMEM cell culture media and incubated for 24 h. Lipidoid nanoparticles were then added into each well. The cells were incubated for another 24 h at 37 °C and 5% CO_2 before MTT reagent (5 mg/mL; in 30 μL PBS) was added. After 4 h incubation, the culture medium was carefully removed and 200 μL of DMSO was added to each well. After dissolving the formazan with DMSO solution, the absorbance at 570 nm was determined using a microplate reader (Molecular Devices Spectra Max).

Statistical Analysis. Data were reported as mean ± SD. Experiments were repeated at least three times. Student's *t* tests were performed to determine the significance of differences between groups. *P* values less than 0.05 were considered to be statistically significant.

■ ASSOCIATED CONTENT

Supporting Information

The Supporting Information is available free of charge at https://pubs.acs.org/doi/10.1021/acs.bioconjchem.0c00295.

Synthetic route, NMR, ESI-MS spectra, TEM images (PDF)

■ AUTHOR INFORMATION

Corresponding Author

Qiaobing Xu − *Department of Biomedical Engineering, Tufts University, Medford, Massachusetts 02155, United States;* orcid.org/0000-0001-7323-7795; Phone: +1 617-627-4322; Email: Qiaobing.Xu@tufts.edu; Fax: +1 617-627-3231

Authors

Yamin Li − *Department of Biomedical Engineering, Tufts University, Medford, Massachusetts 02155, United States;* orcid.org/0000-0002-5535-1807

Raissa Li − *Department of Biomedical Engineering, Tufts University, Medford, Massachusetts 02155, United States*

Anirban Chakraborty − *Department of Biomedical Engineering, Tufts University, Medford, Massachusetts 02155, United States*

Roza Ogurlu − *Department of Biomedical Engineering, Tufts University, Medford, Massachusetts 02155, United States*

Xuewei Zhao − *Department of Biomedical Engineering, Tufts University, Medford, Massachusetts 02155, United States*

Jinjin Chen − *Department of Biomedical Engineering, Tufts University, Medford, Massachusetts 02155, United States*

Complete contact information is available at: https://pubs.acs.org/10.1021/acs.bioconjchem.0c00295

Author Contributions

#R.L. and A.C. contributed equally.

Notes

The authors declare no competing financial interest.

■ ACKNOWLEDGMENTS

This work was supported by National Science Foundation (NSF) Grant DMR1452122 and National Institutes of Health (NIH) Grants R01 EB027170-01 and UG3 TR002636-01.

■ REFERENCES

(1) Altinoglu, S., Wang, M., and Xu, Q. B. (2015) Combinatorial library strategies for synthesis of cationic lipid-like nanoparticles and their potential medical applications. *Nanomedicine 10*, 643−657.

(2) Chang, J., Chen, X. H., Glass, Z., Gao, F., Mao, L. Q., Wang, M., and Xu, Q. B. (2019) Integrating Combinatorial Lipid Nanoparticle and Chemically Modified Protein for Intracellular Delivery and Genome Editing. *Acc. Chem. Res. 52*, 665−675.

(3) Love, K. T., Mahon, K. P., Levins, C. G., Whitehead, K. A., Querbes, W., Dorkin, J. R., Qin, J., Cantley, W., Qin, L. L., Racie, T., et al. (2010) Lipid-like materials for low-dose, in vivo gene silencing. *Proc. Natl. Acad. Sci. U. S. A. 107*, 1864−1869.

(4) Li, Y. M., Chakraborty, A., Chen, J. J., and Xu, Q. B. (2019) Combinatorial Library of Light-Cleavable Lipidoid Nanoparticles for Intracellular Drug Delivery. *ACS Biomater. Sci. Eng. 5*, 2391−2398.

(5) Zhang, C., Zhao, W., Bian, C., Hou, X., Deng, B., McComb, D. W., Chen, X., and Dong, Y. (2019) Antibiotic-Derived Lipid Nanoparticles to Treat Intracellular Staphylococcus aureus. *ACS applied bio materials 2*, 1270−1277.

(6) Liu, F., Yang, L., Li, Y. M., Junier, A., Ma, F. H., Chen, J. J., Han, H. B., Glass, Z., Zhao, X. W., Kumamoto, C. A., et al. (2020) In Vitro and

In Vivo Study of Amphotericin B Formulation with Quaternized Bioreducible Lipidoids. *ACS Biomater. Sci. Eng. 6*, 1064−1073.
(7) Wang, M., Alberti, K., Sun, S., Arellano, C. L., and Xu, Q. B. (2014) Combinatorially Designed Lipid-like Nanoparticles for Intracellular Delivery of Cytotoxic Protein for Cancer Therapy. *Angew. Chem., Int. Ed. 53*, 2893−2898.
(8) Li, Y. M., Yang, T., Yu, Y. J., Shi, N., Yang, L., Glass, Z., Bolinger, J., Finkel, I. J., Li, W. H., and Xu, Q. B. (2018) Combinatorial library of chalcogen-containing lipidoids for intracellular delivery of genome-editing proteins. *Biomaterials 178*, 652−662.
(9) Hou, X. C., Zhang, X. F., Zhao, W. Y., Zeng, C. X., Deng, B. B., McComb, D. W., Du, S., Zhang, C. X., Li, W. Q., and Dong, Y. Z. (2020) Vitamin lipid nanoparticles enable adoptive macrophage transfer for the treatment of multidrug-resistant bacterial sepsis. *Nat. Nanotechnol. 15*, 41−46.
(10) Lamson, N. G., Berger, A., Fein, K. C., and Whitehead, K. A. (2020) Anionic nanoparticles enable the oral delivery of proteins by enhancing intestinal permeability. *Nat. Biomed Eng. 4*, 84−96.
(11) Li, Y. M., Li, A. C., and Xu, Q. B. (2019) Intracellular Delivery of His-Tagged Genome-Editing Proteins Enabled by Nitrilotriacetic Acid-Containing Lipidoid Nanoparticles. *Adv. Healthcare Mater. 8*, 1800996.
(12) Cheng, Q., Wei, T., Farbiak, L., Johnson, L. T., Dilliard, S. A., and Siegwart, D. J. (2020) Selective organ targeting (SORT) nanoparticles for tissue-specific mRNA delivery and CRISPR-Cas gene editing. *Nat. Nanotechnol. 15*, 313−320.
(13) Gao, X., Tao, Y., Lamas, V., Huang, M. Q., Yeh, W. H., Pan, B. F., Hu, Y. J., Hu, J. H., Thompson, D. B., Shu, Y. L., et al. (2018) Treatment of autosomal dominant hearing loss by in vivo delivery of genome editing agents. *Nature 553*, 217−221.
(14) Molla, M. R., Chakraborty, S., Munoz Sagredo, L., Drechsler, M., Orian Rousseau, V., and Levkin, P. A. (2020) Combinatorial Synthesis of a Lipidoid Library by Thiolactone Chemistry: In Vitro Screening and In Vivo Validation for siRNA Delivery. *Bioconjugate Chem. 31*, 852−860.
(15) Zhang, Y. M., Huang, Z., Wu, X. R., Zhang, J., Liu, Y. H., and Yu, X. Q. (2018) Small Combinatorial Library of Lipidoids as Nanovectors for Gene Delivery. *Acs Appl. Nano Mater. 1*, 3925−3934.
(16) Akinc, A., Zumbuehl, A., Goldberg, M., Leshchiner, E. S., Busini, V., Hossain, N., Bacallado, S. A., Nguyen, D. N., Fuller, J., Alvarez, R., et al. (2008) A combinatorial library of lipid-like materials for delivery of RNAi therapeutics. *Nat. Biotechnol. 26*, 561−569.
(17) Hajj, K. A., Ball, R. L., Deluty, S. B., Singh, S. R., Strelkova, D., Knapp, C. M., and Whitehead, K. A. (2019) Branched-Tail Lipid Nanoparticles Potently Deliver mRNA In Vivo due to Enhanced Ionization at Endosomal pH. *Small 15*, e1805097.
(18) Kauffman, K. J., Dorkin, J. R., Yang, J. H., Heartlein, M. W., DeRosa, F., Mir, F. F., Fenton, O. S., and Anderson, D. G. (2015) Optimization of Lipid Nanoparticle Formulations for mRNA Delivery in Vivo with Fractional Factorial and Definitive Screening Designs. *Nano Lett. 15*, 7300−7306.
(19) Lokugamage, M. P., Sago, C. D., Gan, Z. B., Krupczak, B. R., and Dahlman, J. E. (2019) Constrained Nanoparticles Deliver siRNA and sgRNA to T Cells In Vivo without Targeting Ligands. *Adv. Mater. 31*, 1902251.
(20) Whitehead, K. A., Dorkin, J. R., Vegas, A. J., Chang, P. H., Veiseh, O., Matthews, J., Fenton, O. S., Zhang, Y. L., Olejnik, K. T., Yesilyurt, V., et al. (2014) Degradable lipid nanoparticles with predictable in vivo siRNA delivery activity. *Nat. Commun. 5*, 4277.
(21) Li, Y. M., Bolinger, J., Yu, Y. J., Glass, Z., Shi, N., Yang, L., Wang, M., and Xu, Q. B. (2019) Intracellular delivery and biodistribution study of CRISPR/Cas9 ribonucleoprotein loaded bioreducible lipidoid nanoparticles. *Biomater. Sci. 7*, 596−606.
(22) Wang, M., Alberti, K., Varone, A., Pouli, D., Georgakoudi, I., and Xu, Q. B. (2014) Enhanced Intracellular siRNA Delivery using Bioreducible Lipid-Like Nanoparticles. *Adv. Healthcare Mater. 3*, 1398−1403.
(23) Wang, L., Liu, G. H., Wang, X. R., Hu, J. M., Zhang, G. Y., and Liu, S. Y. (2015) Acid-Disintegratable Polymersomes of pH-Responsive Amphiphilic Diblock Copolymers for Intracellular Drug Delivery. *Macromolecules 48*, 7262−7272.
(24) Kanamala, M., Wilson, W. R., Yang, M., Palmer, B. D., and Wu, Z. (2016) Mechanisms and biomaterials in pH-responsive tumour targeted drug delivery: A review. *Biomaterials 85*, 152−67.
(25) Kocak, G., Tuncer, C., and Butun, V. (2017) pH-Responsive polymers. *Polym. Chem. 8*, 144−176.
(26) Gillies, E. R., and Frechet, J. M. J. (2005) pH-responsive copolymer assemblies for controlled release of doxorubicin. *Bioconjugate Chem. 16*, 361−368.
(27) Zhan, L., Chang, S. Y., Liu, T., Yu, S. B., Li, H., Lu, M. J., Zhu, Y., Luo, Y., Yu, J. H., Yang, F., et al. (2017) A new type of pH-sensitive phospholipid. *Tetrahedron Lett. 58*, 4724−4727.
(28) Gujrati, M., Vaidya, A., and Lu, Z. R. (2016) Multifunctional pH-Sensitive Amino Lipids for siRNA Delivery. *Bioconjugate Chem. 27*, 19−35.
(29) Chen, T., Yu, H., Yang, N. E., Wang, M. D., Ding, C. D., and Fu, J. J. (2014) Graphene quantum dot-capped mesoporous silica nanoparticles through an acid-cleavable acetal bond for intracellular drug delivery and imaging. *J. Mater. Chem. B 2*, 4979−4982.
(30) Yang, K. N., Zhang, C. Q., Wang, W., Wang, P. C., Zhou, J. P., and Liang, X. J. (2014) pH-responsive mesoporous silica nanoparticles employed in controlled drug delivery systems for cancer treatment. *Cancer biology & medicine 11*, 34−43.
(31) Kalia, J., and Raines, R. T. (2008) Hydrolytic stability of hydrazones and oximes. *Angew. Chem., Int. Ed. 47*, 7523−7526.
(32) Liu, B., and Thayumanavan, S. (2017) Substituent Effects on the pH Sensitivity of Acetals and Ketals and Their Correlation with Encapsulation Stability in Polymeric Nanogels. *J. Am. Chem. Soc. 139*, 2306−2317.
(33) Deirram, N., Zhang, C. H., Kermaniyan, S. S., Johnston, A. P. R., and Such, G. K. (2019) pH-Responsive Polymer Nanoparticles for Drug Delivery. *Macromol. Rapid Commun. 40*, 1800917.
(34) Kanamala, M., Wilson, W. R., Yang, M. M., Palmer, B. D., and Wu, Z. M. (2016) Mechanisms and biomaterials in pH-responsive tumour targeted drug delivery: A review. *Biomaterials 85*, 152−167.
(35) Griset, A. P., Walpole, J., Liu, R., Gaffey, A., Colson, Y. L., and Grinstaff, M. W. (2009) Expansile Nanoparticles: Synthesis, Characterization, and in Vivo Efficacy of an Acid-Responsive Polymeric Drug Delivery System. *J. Am. Chem. Soc. 131*, 2469−2471.
(36) Gillies, E. R., Goodwin, A. P., and Frechet, J. M. J. (2004) Acetals as pH-sensitive linkages for drug delivery. *Bioconjugate Chem. 15*, 1254−1263.
(37) Gu, Y. W., Ma, J. J., Fu, Z. Q., Xu, Y. F., Gao, B. A., Yao, J. Z., Xu, W., Chu, K. D., and Chen, J. M. (2019) Development Of Novel Liposome-Encapsulated Combretastatin A4 Acylated Derivatives: Prodrug Approach For Improving Antitumor Efficacy. *Int. J. Nanomed. 14*, 8805−8818.
(38) Li, P., Chen, S. M., Jiang, Y. H., Jiang, J. Y., Zhang, Z. R., and Sun, X. (2013) Dendritic cell targeted liposomes-protamine-DNA complexes mediated by synthetic mannosylated cholestrol as a potential carrier for DNA vaccine. *Nanotechnology 24*, 295101.
(39) Zhu, Y., Wang, M. M., Zhang, J. J., Peng, W., Firempong, C. K., Deng, W. W., Wang, Q. L., Wang, S. C., Shi, F., Yu, J. N., et al. (2015) Improved oral bioavailability of capsaicin via liposomal nanoformulation: preparation, in vitro drug release and pharmacokinetics in rats. *Arch. Pharmacal Res. 38*, 512−521.
(40) Antonietti, M., and Forster, S. (2003) Vesicles and liposomes: A self-assembly principle beyond lipids. *Adv. Mater. 15*, 1323−1333.
(41) Israelachvili, J. N., Mitchell, D. J., and Ninham, B. W. (1977) Theory Of Self-Assembly Of Lipid Bilayers And Vesicles. *Biochim. Biophys. Acta, Biomembr. 470*, 185−201.
(42) Jahn, A., Vreeland, W. N., DeVoe, D. L., Locascio, L. E., and Gaitan, M. (2007) Microfluidic directed formation of liposomes of controlled size. *Langmuir 23*, 6289−6293.
(43) Olson, F., Hunt, C. A., Szoka, F. C., Vail, W. J., and Papahadjopoulos, D. (1979) Preparation Of Liposomes Of Defined Size Distribution by Extrusion Through Polycarbonate Membranes. *Biochim. Biophys. Acta, Biomembr. 557*, 9−23.

https://dx.doi.org/10.1021/acs.bioconjchem.0c00295
Bioconjugate Chem. 2020, 31, 1835−1843

(44) Li, Y. M., Liu, G. H., Wang, X. R., Hu, J. M., and Liu, S. Y. (2016) Enzyme-Responsive Polymeric Vesicles for Bacterial-Strain-Selective Delivery of Antimicrobial Agents. *Angew. Chem., Int. Ed. 55*, 1760−1764.
(45) Li, Y. M., Qian, Y. F., Liu, T., Zhang, G. Y., and Liu, S. Y. (2012) Light-Triggered Concomitant Enhancement of Magnetic Resonance Imaging Contrast Performance and Drug Release Rate of Function-alized Amphiphilic Diblock Copolymer Micelles. *Biomacromolecules 13*, 3877−3886.
(46) Kulkarni, J. A., Cullis, P. R., and van der Meel, R. (2018) Lipid Nanoparticles Enabling Gene Therapies: From Concepts to Clinical Utility. *Nucleic Acid Ther. 28*, 146−157.
(47) Sago, C. D., Lokugamage, M. P., Paunovska, K., Vanover, D. A., Monaco, C. M., Shah, N. N., Gamboa Castro, M., Anderson, S. E., Rudoltz, T. G., Lando, G. N., et al. (2018) High-throughput in vivo screen of functional mRNA delivery identifies nanoparticles for endothelial cell gene editing. *Proc. Natl. Acad. Sci. U. S. A. 115*, E9944−E9952.
(48) Cheng, X., and Lee, R. J. (2016) The role of helper lipids in lipid nanoparticles (LNPs) designed for oligonucleotide delivery. *Adv. Drug Delivery Rev. 99*, 129−137.
(49) Du, Z., Munye, M. M., Tagalakis, A. D., Manunta, M. D., and Hart, S. L. (2015) The role of the helper lipid on the DNA transfection efficiency of lipopolyplex formulations. *Sci. Rep. 4*, 7107.
(50) Li, Y., Jarvis, R., Zhu, K., Glass, Z., Ogurlu, R., Gao, P., Li, P., Chen, J., Yu, Y., Yang, Y., et al. (2020) Protein and mRNA Delivery Enabled by Cholesteryl-Based Biodegradable Lipidoid Nanoparticles. *Angew. Chem., Int. Ed.*, DOI: 10.1002/anie.202004994.
(51) Sun, S., Wang, M., Alberti, K. A., Choy, A., and Xu, Q. (2013) DOPE facilitates quaternized lipidoids (QLDs) for in vitro DNA delivery. *Nanomedicine 9*, 849−54.
(52) Hajj, K. A., and Whitehead, K. A. (2017) Tools for translation: non-viral materials for therapeutic mRNA delivery. *Nat. Rev. Mater. 2*, 17056.
(53) Weissman, D., and Kariko, K. (2015) mRNA: Fulfilling the Promise of Gene Therapy. *Mol. Ther. 23*, 1416−1417.

https://dx.doi.org/10.1021/acs.bioconjchem.0c00295
Bioconjugate Chem. 2020, 31, 1835−1843